



# Modification of graphene for speciation of chromium in wastewater samples by suspension solid phase microextraction procedure

Ahmad Ghozatloo<sup>a,\*</sup>

<sup>a,\*</sup> Research Institute of Petroleum Industry (RIPI), West Blvd. Azadi Sport Complex, P.O. Box: 14665-137, Tehran, Iran

## ARTICLE INFO:

Received 30 Jun 2019

Revised form 28 Jul 2019

Accepted 30 Aug 2019

Available online 26 Sep 2019

## Keywords:

Chromium,  
Extraction,  
Graphene,  
Modified graphene,  
Sulfonated and Amidation,  
Environment sample

## ABSTRACT

In this study, the surface modification of graphene (SMG) was developed for efficient speciation and determination of chromium in water and wastewater samples. First surface of the graphene was modified with acid mixtures, potassium persulfate (KPS) in an alkaline media, tetra hydro furan (THF), Octadecyl amine and sodium dodecyl benzene sulfonate (SDBS) as synthesis. By procedure, the chromium ions was extracted from water/wastewater sample based on sulfonated and amine graphene (S-NG, N-NG) by suspension solid phase microextraction procedure (SMSPE). Hydrophobic ionic liquid ([HMIM] [PF<sub>6</sub>]) was used for separation graphene from 10 mL of waters. After shaking and centrifuging, the phase of Cr→S-NG, Cr→N-NG was back extracted by 0.2 mL of HNO<sub>3</sub> (0.4 mol L<sup>-1</sup>) and finally chromium concentration determined with electrothermal atomic absorption spectrometry (ET-AAS). The results showed, the sulfonated and amine graphene can successfully extracted Cr(III) and Cr(VI) from water and wastewater samples at pH=3.5-5.5 and pH<3, respectively. Also, the most Cr(VI) extracted by N-graphene at pH=2(NH<sub>3</sub><sup>+</sup>→Cr<sub>2</sub>O<sub>7</sub><sup>-</sup>). Under the optimal conditions, the linear range, limit of detection and preconcentration factor were obtained 0.02–2.4 μg L<sup>-1</sup>, 5.0 ng L<sup>-1</sup> and 20.2 for 10 mL of water samples, respectively for Cr(III,VI) (%RSD<5%, pH=4). The validation of methodology for speciation of chromium was confirmed by spiking real samples.

## 1. Introduction

Different synthesis of graphene was used for extraction metals from waters [1]. Novel materials, such as graphene with various structures, have numerous advantages that make them favorable for many analytical chemistry applications [2]. Because of inherent low coefficient thermal expansion of graphene and its lightweight, high thermal and mechanical properties and ease for nanocomposites, it has been widely used in aqua phase materials such as water and wastewater samples [3]. Then

grapheme sheets have been used for extraction metals and VOCs. As solid phase extraction (SPE) with graphene, it is big to be dispersed in solution and cannot too long dispersion in polar solvents. Also, graphene nano sheets was hold together in bundles by van der Waals interactions [4, 5]. The grapheme nano sheets are hydrophobic and thus have a non-homogeneous form in water, so, simply used for heavy metal extraction as physical adsorption. But chemical methods involve surface modification of graphene for chemical bonding between graphene and function group. Surface control of nano particles to receive semi or full hydrophilic or hydrophobic properties has attracted

\*Corresponding Author. Ahmad Ghozatloo

E-mail: [ghozatloo@ripi.ir](mailto:ghozatloo@ripi.ir)

<https://doi.org/10.24200/amecj.v2.i03.67>

extensive research interests over the few years due to its importance in chemistry research and potential applications such as extraction ions from different matrixes. All the existing modification methods of graphene for chemical applications are wet-chemical method [6-7]. As synthesis of graphene modification, carboxylic acid, hydroxyl, nitrogen and sulfur group are the most common functional groups for absorption analysis [8]. Although this approach can increase the dispersion property but it can also have a detrimental effect on the conductivity of the composites and nano fluids [9]. Surfactants have also been used to disperse nanostructures, since this prevents them from becoming aggregated over time [10].

The wide application exists for modification of graphene specially sulfonated and amidation graphene (S...NG, N...NG). Recently, metal extraction occurred with graphene and modification graphene in water, human matrix and foods. Some toxic metal such as mercury, chromium and lead in drinking water and human blood or serum cause physiological or neuro-logical damage in human body. Chromium, specially Cr(VI) is a toxic pollutant in the environment, industries and factories. Cr determination in human body and waters is important because of health problem such as chromosome aberration, mutations, and carcinogenicity in cells. So, ultra-trace determination of Cr is very important in water samples. Many methods developed for Cr extraction in water samples by graphene sorbents. Cr enter the human body through food or drinking water, and its level in the air, water and biological samples is very low. Cr concentration in drinking water is generally less than  $2\text{ g L}^{-1}$ . The World Health Organization (WHO) states that the guideline values of  $50\text{ g L}^{-1}$  for Cr (VI) is considered as high concentration value in human [11-14]. In this paper, the extraction recovery and absorption capacity of different functionalized graphene for chromium was calculated by SMSPE procedure after synthesis. Also, the behavior of different functionalized graphene for extraction of chromium was investigated and compared together.

The sulfonated (:S<sup>-</sup>-NG) and amine graphene (:N<sup>+</sup>-NG) was used for extraction cations of Cr(III)<sup>+</sup> and anions of Cr(VI)<sup>-</sup> from water and wastewater samples at pH=4 and pH=2, respectively. Other compounds have low extraction efficiency as compared to (:S-NG) and (:N-NG).

## 2. Experimental

### 2.1. Chemical materials

In the present work, acetone, toluene, Thionyl Chloride (SOCl<sub>2</sub>) >98%, potassium persulphate (KPS) >99.9% and Sodium hydride (NaH)>90% obtained from Sigma-Aldrich. Also Methyl ethanesulfonate (C<sub>3</sub>H<sub>8</sub>O<sub>3</sub>S) >97%, Ethylmethylaniline (C<sub>3</sub>H<sub>9</sub>N)>98% and Sodium 2-dodecylbenzenesulfonate (SDBS) obtained from ChemSpider. The reagents such as; HNO<sub>3</sub>, H<sub>2</sub>SO<sub>4</sub>, HCl, NaOH, KOH, as analytical grade were purchased from Internal Companies, Iran. Deionized water was purchased from Bahre-e Zolal-e Tehran Company.

### 2.2. Synthesized and Characterization of Graphene

Graphene was synthesized by chemical vapor deposition (CVD) with methane as a carbon feed under hydrogen atmosphere at 1100°C [15]. Provided graphene is pure with nano sheet structure. The CVD graphene was characterized with X-ray diffraction (XRD) and TEM imaging. X-ray diffraction measurements were carried out using a X-pert Philips diffractometer equipped with a CuK $\alpha$  source (wavelength  $\lambda = 0.154\text{ nm}$ ). The XRD pattern of CVD graphene was shown in Figure 1. As shown in Figure 1, one high-intensity broad peak was appear about  $2\theta=26.5$  corresponding to (002) diffraction line (d-space 3.4Å) plane of graphite. It was proved the pure and crystalline of CVD graphene structure [16]. By using Scherrer equation, the crystalline size of graphene is calculated as 1.8 nm and when it is divided by the distance of graphene layers (3.4 Å), the number of graphene sheets is calculated as 5.3 layers. In order to evaluate the morphology and diameter distribution of the graphene, TEM image was taken for the pristine graphene of CVD. Transmission

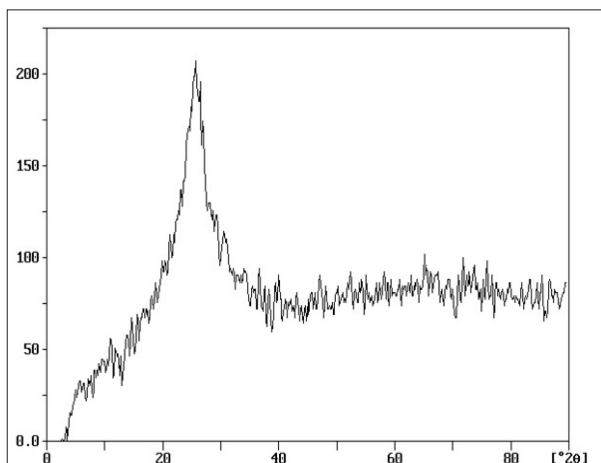


**Fig. 1.** XRD patterns of CVD Graphene

Electron Microscopy (TEM) was carried out using a ZEISS EM900 KNL groups at 100kV. The TEM image of CVD graphene was shown in Figure 2. It exhibits a high magnification TEM image of CVD graphene, showing a completely sheet structure and ordered with few layers [17].

### 2.3. Surface modification methods for graphene

The main motive of this paper is to provide a framework for using an appropriate functional group from the upcoming options when using graphene nanofluids. Surfactant treatment was used as surface modification methods. Surfactant has been used to disperse graphene, since this prevents them from becoming aggregated over time [18]. These treatments improve the dispersion of graphene in aqueous media. To improve graphene dispersion in water the sheets were dispersed with the aid of SDBS surfactant as follows [19]. The samples formed from graphene treated with SDBS were designated as SDBS-GNSs. The reaction scheme for the treatment of graphene using SDBS shows in Figure 3 (a). Also, basic treatment was used as another way for surface modification methods. For basic treatment, the surface modification of graphene was performed with KPS at 100°C refluxed for 8 hr. as follows [20]. The samples formed from graphene treated with basic method were designated as K-GNSs. The reaction scheme for the treatment of graphene using KPS shows



**Fig. 2.** TEM image of CVD Graphene

in Figure 3(b). In addition, surface modification methods flowed by K-GNSs which were treated with SDBS for 24 h at room temperature to obtain surfactant treated K-GNSs [21]. The samples formed from K-GNSs treated with SDBS were designated as SDBS-KGNS. Figure 3(c) gives a schematic diagram of the process of the SDBS-KGNSs. In order to achieve the highest stability, the amount of consumed SDBS was considered twice as much as graphene amount in the fluid. Acid treatment and surfactant based acid treatment were used for functionalized graphene. For acid treatment, the surface modification of graphene was performed with 1:3 mixtures of concentrated  $\text{HNO}_3$  and  $\text{H}_2\text{SO}_4$  at 60 °C for 3 hr. as follows [22]. The samples formed from graphene treated with acid mixture were designated as A-GNSs. The reaction scheme for the treatment of graphene using Acid treatment shows in 3(d). For surfactant – acid treatment, the A-GNSs were treated with SDBS for 24 h at room temperature to obtain surfactant treated A-GNSs as follows [21]. The samples formed from A-GNSs treated with SDBS were designated as SDBS-AGNSs. 3(e) gives a schematic diagram of the process of the SDBS-AGNS. Finally, amidation and sulfate treatment was prepared for this research. For amidation treatment, acyl-chlorinated graphene was added to an amine compound (octa decyl amine). This mixture was sonicated using an ultrasound bath at 70°C for 2

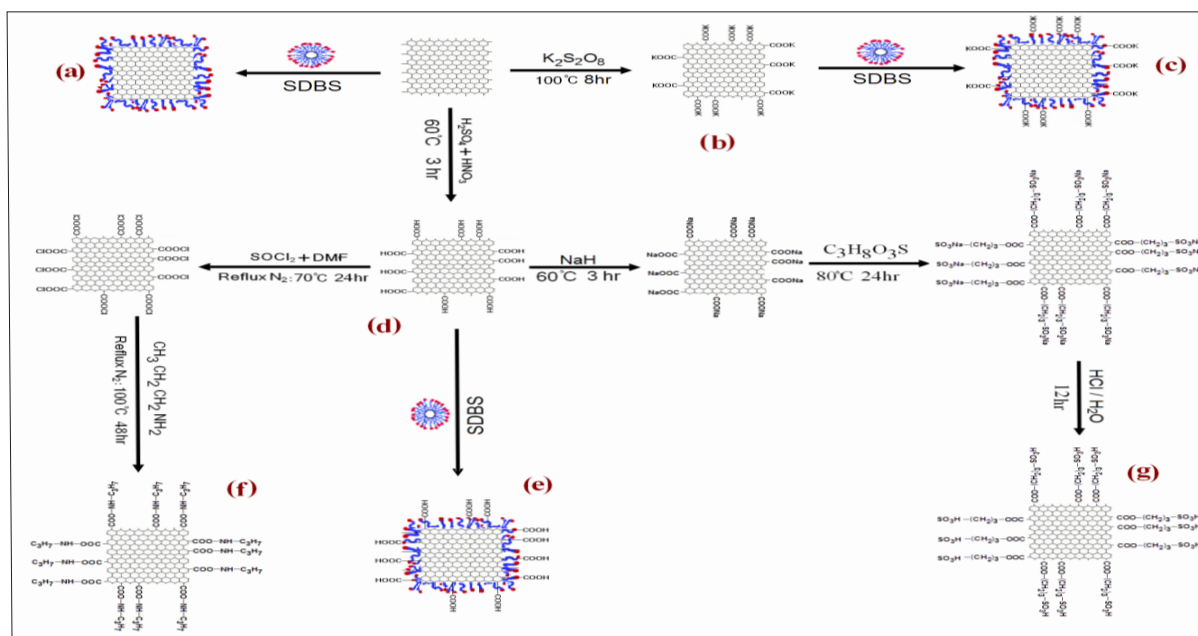


**Fig. 3.** Schematic representations of surface modification of graphene by (a) Surfactant (b) alkaline method (c) Surfactant & alkaline (d) acid media (e) Surfactant & acid (f) Amidation N-NG (g) Sulfate treatment, S-NG

hr, and then refluxed for 2 days. After cooling to room temperature the product were washed with ethanol to remove excess amine. Finally the black solid was dried at 70°C overnight. The samples formed from graphene treated with amidation were designated as :N-NG. Corresponding chemical reactions are illustrated in 3(f) [22]. For sulfate treatment, graphene was added to anhydrous THF under vigorous mechanical stirring. To replace the terminated Na with H in graphene, sodium hydride (NaH) was added slowly to the graphene/THF mixture at 60°C for 6 hr. Propane sultone was then added drop wise to the mixture, and this mixture was reacted at 80°C for 24 hr. with constant stirring. After the reaction, filtered reactant was immersed into an HCl/water solution for 12 h and then washed with ethanol several times to remove the residuals. The product was dried in vacuum at 70°C for 6 hr. [23]. The samples formed from graphene treated with Sulfate treatment were designated as :S-NG. 3(g) gives a schematic diagram of the sulfonation process of the sulfonated graphene.

#### 2.4. General Procedure

Chromium was separated and determined based on functionalized graphene (S-NG, N-NG) from

water sample with SMSPE coupled by ETAAS. For speciation of chromium, 20 mg of N-NG/S-NG dispersed in 10 mL of standard and water sample at pH=4 and pH=2 for complexation with sulfur and amide group for extraction cations of Cr(III)<sup>+</sup> and anions of Cr(VI)<sup>-</sup> from water and wastewater samples. After shaking and centrifuging processes, the Cr(III) and Cr(VI) complexation was achieved [Cr<sub>III</sub>→:S-NG, Cr<sub>VI</sub>→:N-NG] and trapped with [HMIM][PF6] in conical tube. Then, the chromium in remained IL/sorbent back extracted by 0.2 mL of HNO<sub>3</sub> (0.4 mol L<sup>-1</sup>)/ NaOH(0.2 M) and finally Cr(III) and Cr(VI) concentration determined with ET-AAS after dilution with DW up to 1 mL. The results showed us, the Cr(III) and Cr(VI) can be extracted by S-NG at and N-NG at pH=4 and pH=2, then back extracted by HNO<sub>3</sub> and NaOH. The validation of methodology was confirmed by spiking chromium standard solution and certified reference materials in water (SRM). The optimized conditions were shown in Table 1.

### 3. Results and Discussion

All parameters for chromium extraction was studied and optimized by graphene sorbents by ET-AAS. The results showed that. The sulfur and amide group

**Table 1.** The conditions for chromium extraction based on S-NG /IL and N-NG/IL by SMSPE procedure ( $\mu\text{g L}^{-1}$ )

Factor	Water	Standard
PF <sup>a</sup>	20.2	20.4
LOD <sup>b</sup>	0.005	0.0045
%RSD <sup>c</sup>	3.9	3.2
Linear range	0.02 – 2.2	0.02 – 2.1
Correlation coefficient	0.9992	0.9996

<sup>a</sup> Preconcentration factor<sup>b</sup> Limit of detection<sup>c</sup> Relative standard deviation(V=10 mL, n=10).

of graphene was more extraction of chromium from waters as compared to other function group graphene in this study. The matrix effects in water samples were calculated as extracted chromium from a wastewater matrix to extract chromium from Standard solution by SMSPE-ETAAS procedure (Q1). The recovery efficiency (RE) was obtained by equation Q2.

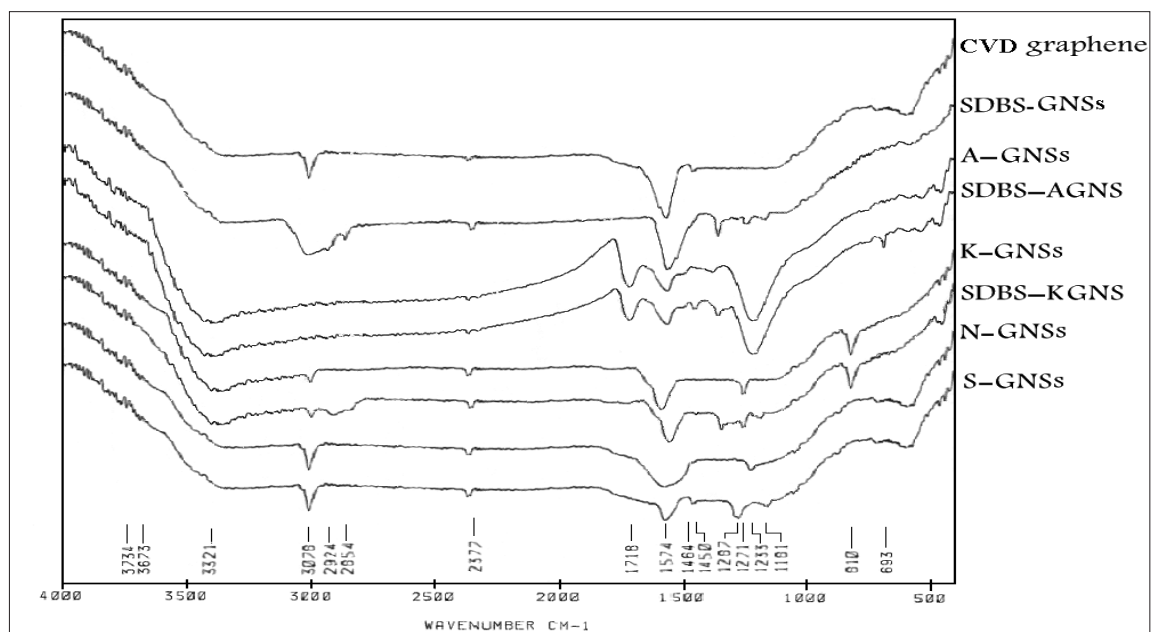
$\% \text{ME} = (\text{Peak area of the Hg extraction in human matrix}) / (\text{Peak area of the Hg extraction in matrix free solution}) \times 100$  (Q1)

$$\text{Recovery \%} = \frac{(C_i - C_f)}{C_i} \times 100 \quad (\text{Q2})$$

### 3.1. FTIR analysis

The presence of variety functional groups were confirmed by FTIR spectra. Therefore in this paper in order to study the structural changes in the

graphene after surface modification, FTIR analysis was performed. FTIR spectrometer (Thermo Scientific, Nicolet 6700) was recorded typically 100 scans over the range  $450\text{-}4000\text{cm}^{-1}$  were taken from each sample with a resolution of  $2\text{ cm}^{-1}$  and summed to provide the spectra. Figure 4 shows FTIR spectra for prepared of the functionalized graphene. The peak at  $1574\text{ cm}^{-1}$  corresponds to the FTIR-active phonon mode of the graphene. This spectrum peak is assigned to the (C=C) stretching mode associated with graphene edge defects [24]. Peak of  $1574\text{ cm}^{-1}$  can be attributed aromatic structures [25]. The FTIR spectra of the SDBS treated graphene (SDBS-GNSs, SDBS-AGNSs and SDBS-KGNSs) showed peaks at  $2924\text{ cm}^{-1}$ , which apparently correspond to the symmetrical stretching of  $(\text{CH}_2)$ , at  $1378\text{ cm}^{-1}$  due to the asymmetrical

**Fig. 4.** FTIR spectra for the functional graphene for N-NG (N-GNSs) and S-NG(S-GNSs)

vibration of ( $\text{CH}_3$ ) two peaks at  $1181\text{ cm}^{-1}$  and  $1236\text{ cm}^{-1}$  due to the asymmetrical vibration of (S–O) and (S=O) respectively [26]. These peaks indicate successful adhesive of SDBS on graphene. The broad band of FTIR spectra  $3400\text{ cm}^{-1}$  corresponds to the presence of the oxygenated groups [27]. In addition, the spectra of the A-GNSs showed peak at around  $1718\text{ (C=O)}\text{ cm}^{-1}$ , asymmetric and  $1079\text{ (C-O)}\text{ cm}^{-1}$ , apparently corresponding to the stretching mode of the carboxylic acid group (COOH) [24]. These peaks indicate successful generation of (COOH) groups on graphene. In the case of the oxidized graphene by basic treatment with KPS, the two main peaks observed. A peak in the  $810\text{ cm}^{-1}$  due to the symmetrical stretching of the (C–S) [20], and Peaks of  $1233\text{ cm}^{-1}$ ,  $1572\text{ cm}^{-1}$ ,  $1585\text{ cm}^{-1}$  are associated with resonance of the (C–O), stretching of the (C–O), and stretching of the (C=O) respectively related to (–COOK) groups [18]. Therefore, hydroxyls, carboxylate groups in K-GNSs were formation the graphene have been successfully to K-GNSs. The peak observed at  $1618\text{ cm}^{-1}$  is associated with the (C=O) bond shifted to  $1636\text{ cm}^{-1}$  (amido-functionalized of graphene) [26]. The existence of vibration modes corresponding to (C–N) at  $1287\text{ cm}^{-1}$ , (N–H) at  $1507$  and  $3421\text{ cm}^{-1}$  indicate the formation of the amine bond [28].

In the spectrum of S-AGNSs the two main peaks observed, a peak in  $1271\text{ cm}^{-1}$  and a peak in  $1181\text{ cm}^{-1}$  due to the symmetrical stretching of the (S=O) and (S–O) respectively which have shown typical absorbance for the sulfonic acid groups ( $\text{SO}_3\text{H}$ ) [17].

### 3.2. Raman spectroscopy

Raman spectroscopy is a very valuable tool for the characterization of carbon-based nanostructures and confirmed that the structure how much ruptured after treatment. Raman spectroscopy (Renishaw RM1000 -Invia) was used to investigate graphene structural changes during the surface modification treatments. The ratio between D and G band is a good indicator of the quality on bulk samples and is very important factor in the way that allows distinguishing between the functional graphene samples after treatment with different agents. The degree of functionalization can be estimated by the intensity of the D and G band [19]. Figure 5 shows the Raman spectrum of the samples reported in Table 1.

These typical peaks, which still present after surface treatments were prove the structure of graphene didn't damage during that varies treatments. Generally the ratio of  $I_D/I_G$  is increased

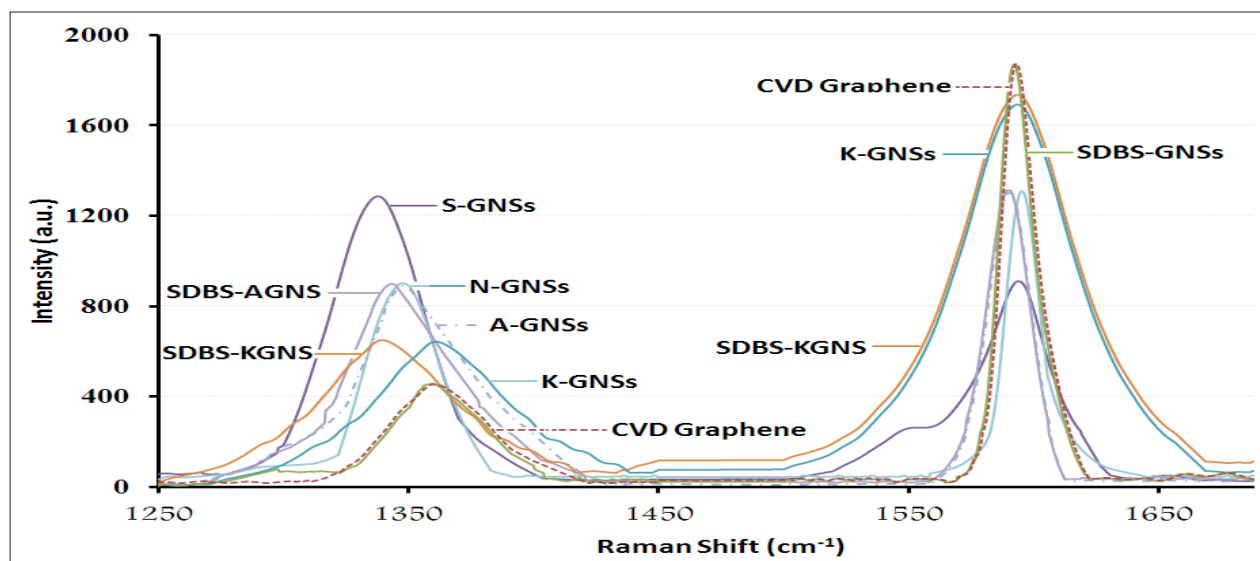


**Fig. 5.** Raman spectra of CVD and Functionalized graphene after treatment with different agents The D band of Raman spectra of CVD graphene is  $1361\text{ cm}^{-1}$  and its intensity ( $I_D$ ) is 455 and the G band is  $1592\text{ cm}^{-1}$  and its intensity ( $I_G$ ) is 1853 so its  $I_D/I_G = 0.246$ .

**Table 2.**  $I_D/I_G$  ratio of the functionalized graphene

Intensity	$I_D$	$I_G$	$I_D/I_G$
CVD graphene	455	1853	0.246
SDBS-GNSs	458	1871	0.245
K-GNSs	641	1691	0.379
SDBS-KGNS	648	1732	0.374
A-GNSs	893	1302	0.686
SDBS-AGNS	898	1312	0.684
N-GNSs	901	1308	0.689
S-GNSs	1288	911	1.414

for functionalized graphene as compared to CVD graphene in all treatment methods. It means that chemical treatments of graphene breaks some bonds and insert functional groups that can be considered as defects on the structure. The  $I_D/I_G$  ratio of functional graphene was summarized in Table 2. Sulfate treatment gave larger  $I_D/I_G$  (1.414) than amidation (0.689) and other method treatment of graphene. The measured intensity  $I_D/I_G$  ratio of the functionalized graphene were in the order of S-GNSs > N-GNSs > A-GNSs > SDBS-AGNS > K-GNSs > SDBS-GNSs.

### 3.3 Preparing and Stability of graphene nanofluids

The dispersion stability of nano structures is an important factor in fabricating uniformly dispersed NFs. The thermal properties of the resulting NFs

will also be strongly influenced by the dispersion stability of graphene. In order to prepare the samples (graphene NFs), two-step process was used. Functionalized graphene with the 0.075wt% mix up with deionized water (DI) and place in the ultrasonic bath (frequency range 20 kHz and power of 80 watts) for 60 min. The specifications of the samples were tabulated on Table 3.

Figure 6 shows the pictures of the functionalized graphene which dispersed in water. Sample (1), includes CVD graphene without any treatment, instability of graphene was observed. Therefore CVD graphene without any treatment has poor dispersion stability in water [29]. Sample (2), includes graphene with SDBS, few aggregations was observed. However, in samples 3~8 good dispersion were observed which functionalized

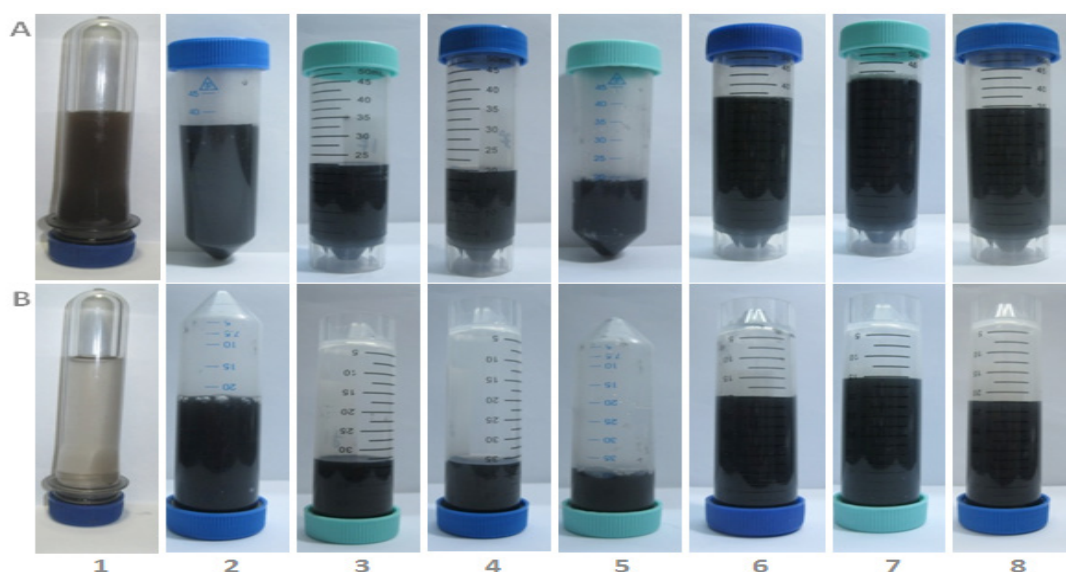


**Fig. 6.** The images of the dispersed graphene in water (a) immediately after sonication, (b) after 7 days (1)CVD graphene, (2)SDBS-GNS, (3)K-GNSs, (4)SDBS-KGNS, (5)A-GNSs, (6)SDBS-AGNS, (7)N-GNSs & (8)S-GNSs

**Table 3.** Specification of 0.075wt% functionalized graphene nanofluids

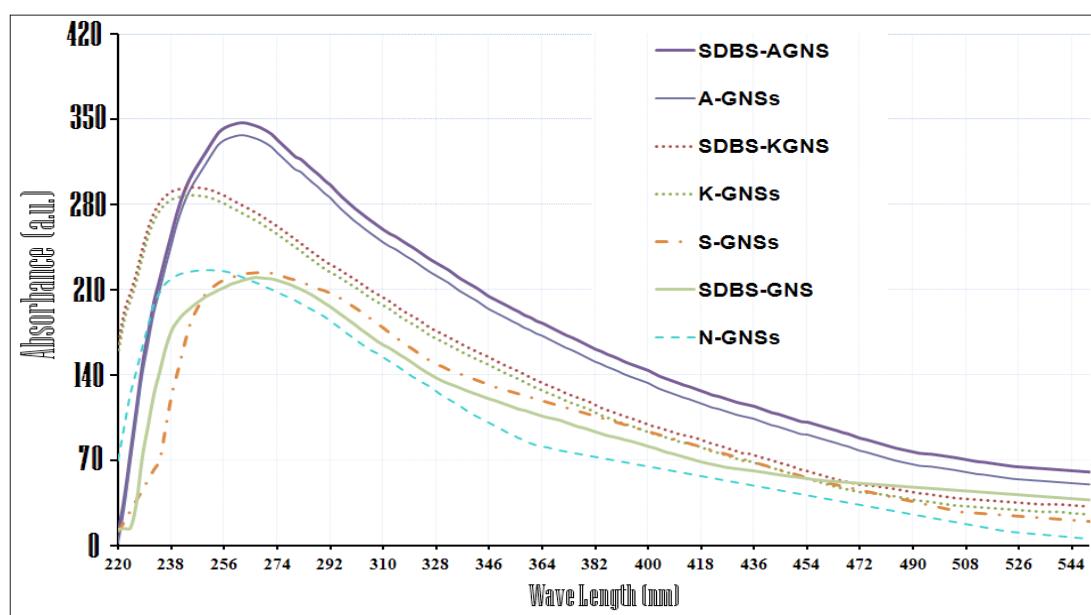
Sample	Nano Structure	Type of Treatment	Type of Agent
1	CVD graphene	-----	-----
2	SDBS-GNSs	Surfactant	SDBS
3	K-GNSs	Alkaline	$K_2S_2O_8$ -KOH
4	SDBS-KGNS	Surfactant - Basic	SDBS- $K_2S_2O_8$
5	A-GNSs	Acid	$H_2SO_4$ - $HNO_3$
6	SDBS-AGNS	Surfactant - Acid	SDBS- $H_2SO_4$
7	N-GNSs	Amine	Octa Decyl Amine
8	S-GNSs	Sulfate	THF-NaH

graphene was used with different treatments.

The results of stability were semi quantified by measuring the absorbance of visible light [30]. The dispersion stability of the surface-modified graphene in water was measured by UV-visible spectroscopy (UVS-2100 SCINCO spectrophotometer between 200 and 1100nm) at ambient temperature. If the nanomaterials dispersed in fluids have characteristic absorption bands in the wavelength 200–1100 nm, it is an easy and reliable method to evaluate the stability of nanofluids using UV-vis spectral analysis. The Samples were diluted up to the extents that were suitable for UV-VIS measurements. Figure 7 shows the peak absorbance of the samples around the range of 220-290 nm. As shown in Figure 7, the high peak of the SDBS-AGNS, A-GNSs show a well dispersion in water. Significant increase in their absorbance

is good agreement (Fig. 7). According to Figure 7, N-CNTs and S-CNTs also show fine dispersion in water. After 7 days, the suspensions were still homogeneous but for the SDBS-GNSs scarcely any sedimentation was observed. This is due to the fact that the defect of the graphene carries more dissociated (-COO) groups, which can stabilize the nano sheets via an electrostatic stabilization mechanism [31].

Furthermore, the SDBS present will act as a self-assembly template. Consequently, functionalized treatments have a different stability and dispersion for graphene in water. The measured dispersion stabilities are in the order of SDBS-AGNS > A-GNSs > SDBS-KGNS > K-GNSs > S-GNSs > SDBS-GNS > N-GNSs. The results showed us, maximum Cr (III) extracted by S-GNSs and extraction efficiency in the order of S-GNSs >

**Fig. 7.** UV-visible spectra of surface-modified graphene nanofluids

SDBS-GNS > SDBS-KGNS> SDBS-AGNS> N-GNSs> K-GNSs, respectively. Also, Cr (VI) extracted by N-GNSs and extraction efficiency in the order N-GNSs> K-GNSs> SDBS-AGNS, respectively.

### 3.4. Thermal conductivity variations vs. temperature

Thermal conductivities of the graphene /water NFs were measured by KD2 Pro thermal properties analyzer (Decagon devices, Inc., USA). The instrument had a specified accuracy of 0.1% and meets the standard of IEEE 442-1981. The instrument had a probe of 60 mm length and 1.3mm diameter, a thermo resistor and a microprocessor to control and measure the conduction in the probe. The instrument had a specified accuracy of 5%. In order to obtain precise results, the sample and the probe were maintained at constant temperature for about 15 min. In order to study the effect of temperature, a thermostat bath was used, which meets the standards of ASTM D5334 at temperature range of 10 to 60. Each data presented is the average value of the measurements from five tested the samples. In general, compare to base fluid, thermal conductivity of NFs is more sensitive due to temperature and increases with increasing of temperature. In order to study the temperature effect on thermal conductivity of the samples a thermostat bath was used. Experimental data were indicate

thermal conductivity of the samples involving functionalized graphene/water NFs increases with temperature and the results were shown in Figure 8. The thermal conductivity of all samples was dramatically increased by the introduction of the graphene. Among the samples, the highest thermal conductivity value (0.728w/mK) was observed for SDBS-KGNS and then (0.704w/mK) K-GNSs.

This may be due to the fact that after their oxidation by the base treatment, the surfaces of graphene contain more function groups. According to Boehm titration, results were observed functional group in alkaline method is about 3%, while the acid treatment is top 5%. Alkaline method usually provides less functional group than acid treatment but provides more stability. It must be noted that alkaline treatment was done in a mild condition, thus the structure of graphene at acid treatment would be more damage than alkaline treatment. Based on Brownian motion of fluids, the functionalized graphene move fast in the water, so that energy transport inside the liquid becomes strong and thermal conductivity increases [33]. Therefore, thermal conductivity gradually ascends in the functionalized graphene /water nano fluids by increasing of temperature. According to Figure 8, by increasing temperature, there are semi linear increases for thermal conductivity of all the samples. For example, thermal conductivity of the

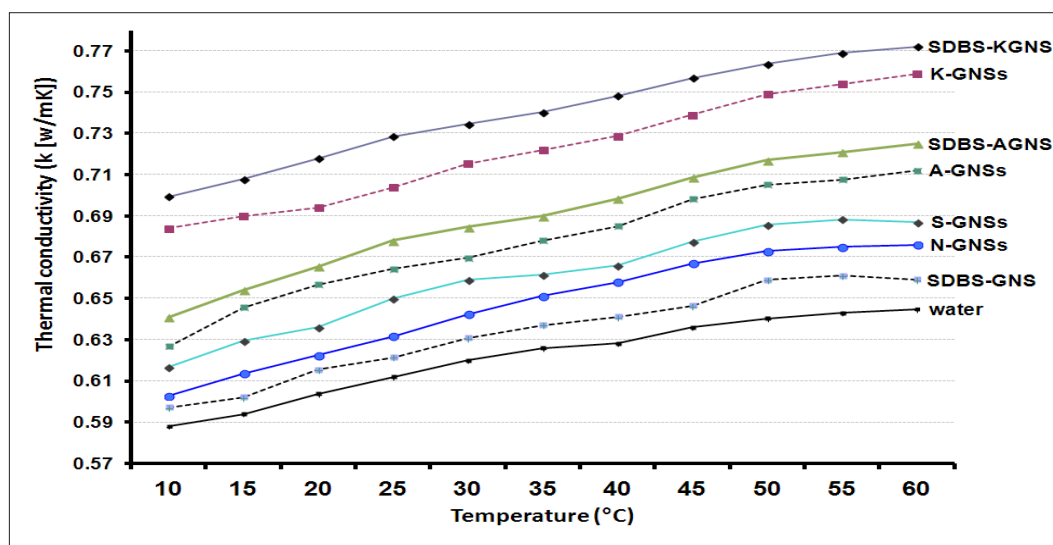


Fig. 8. Thermal Conductivity of the samples vs. Temperature

**Table 4.** Thermal conductivity of 0.1wt% functionalized graphene nanofluids

Samples	nano structure	k @ 25°C		k @ 60°C		Improvement (%)
		(w/m.K)				
1	water	0.612		0.645		5.39
2	SDBS-GNSs	0.621		0.659		6.12
3	K-GNSs	0.704		0.759		7.81
4	SDBS-KGNS	0.728		0.772		6.04
5	A-GNSs	0.664		0.712		7.23
6	SDBS-AGNS	0.678		0.725		6.93
7	N-GNSs	0.632		0.676		6.96
8	S-GNSs	0.650		0.687		5.69

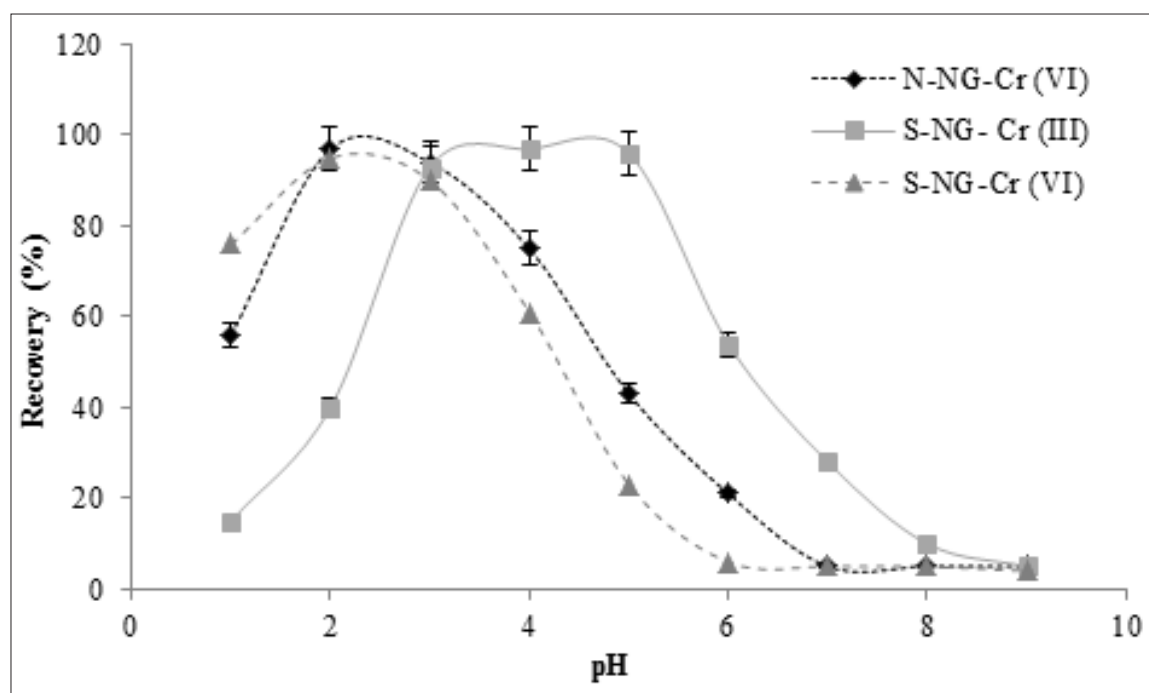
SDBS-KGNS increases about 10.5% at 10 to 60°C and 18.9% enchantment for SDBS-KGNS compare to water at 25°C. Table 4 represents the measured thermal conductivity of 0.1wt% functionalized graphene NFs. For Cr(III) and Cr (VI) analysis with electrochemistry, thermal conductivity is main factor for cyclic voltammetry analysis(CVA) at upper 60°C.

### 3.5 Optimizing of Parameters

The pH of the sample solution is an important factor for quantitative extraction of chromium in waters [34-37]. The pH was affected on surface charge of the graphene or function group of

graphene (FNG) for separation of chromium from liquid phase by SMSPE procedure. So, the effect of sample pH on the chromium recovery by NG and FNG was examined in pH ranges from 1 to 12 by using buffered sample solutions containing 0.2-2  $\mu\text{g L}^{-1}$  of chromium. The recovery of Cr(III) and Cr(VI) extraction for sulfonated (S-NG) and amidation graphene (N-NG) was obtained at pH=4 and pH=2, respectively (more than 96%, Fig. 9). Also, Cr(VI) can be extracted by S-NG at pH=1-3.

Also, the effect of amount of sulfonated and amine graphene (S-NG, N-NG) by ionic liquid [HMIM][PF<sub>6</sub>] for chromium extraction in waters was investigated. The various amounts of S-NG,

**Fig. 9.** The effect of pH on chromium extraction by FNG

N-NG in the ranges of 2 to 30 mg were studied, respectively. Other modified graphene set aside from study because of low efficient recovery as compared to S-NG and N-NG sorbents. The results showed, the amount of 12 mg of both graphene was efficient extracted in present of [HMIM][PF<sub>6</sub>] in waters. So, 15 mg of sorbents were considered as the optimum mass (Fig. 10).

The volume of samples for extraction of chromium was tested by proposed method and 10

mL of sample volume selected for further study (Fig. 11).

Also, some inorganic acid prepared for back extraction of chromium (III) from S-NG was examined and finally, 0.2 mL of HNO<sub>3</sub>, 0.4 mol L<sup>-1</sup> (0.4 M) was obtained by optimizing (Fig. 12). The 0.2 mL of NaOH (0.2 M) used for back extraction of Cr (VI) as optimized reagent for N-NG at pH=2.

The different mass of vary ILs was used for extraction chromium by S-NG, N-NG. In

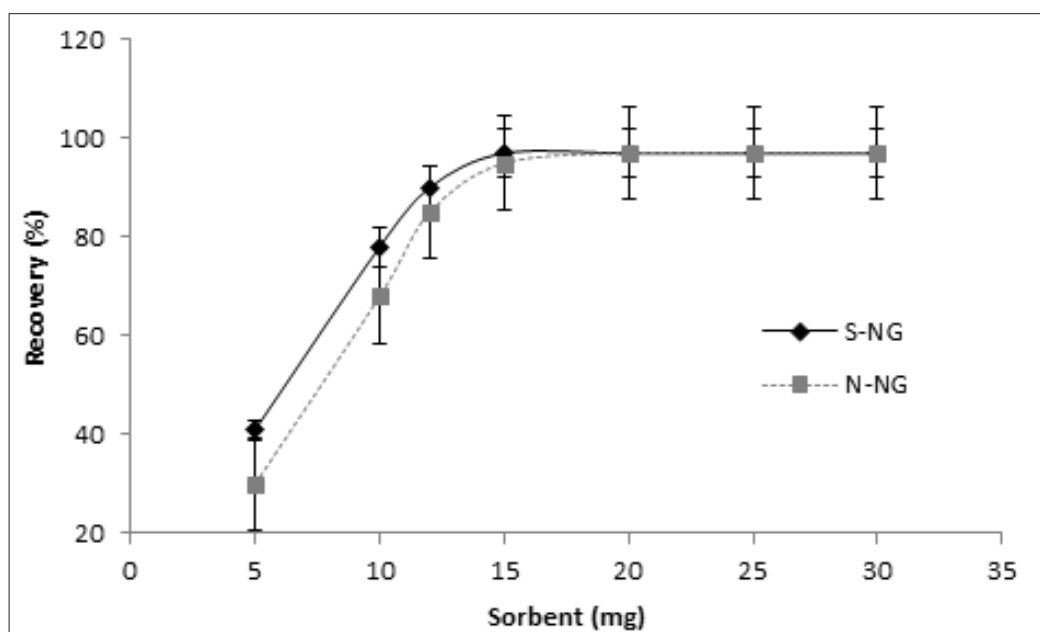


Fig. 10. The effect of amount of FNG on chromium extraction

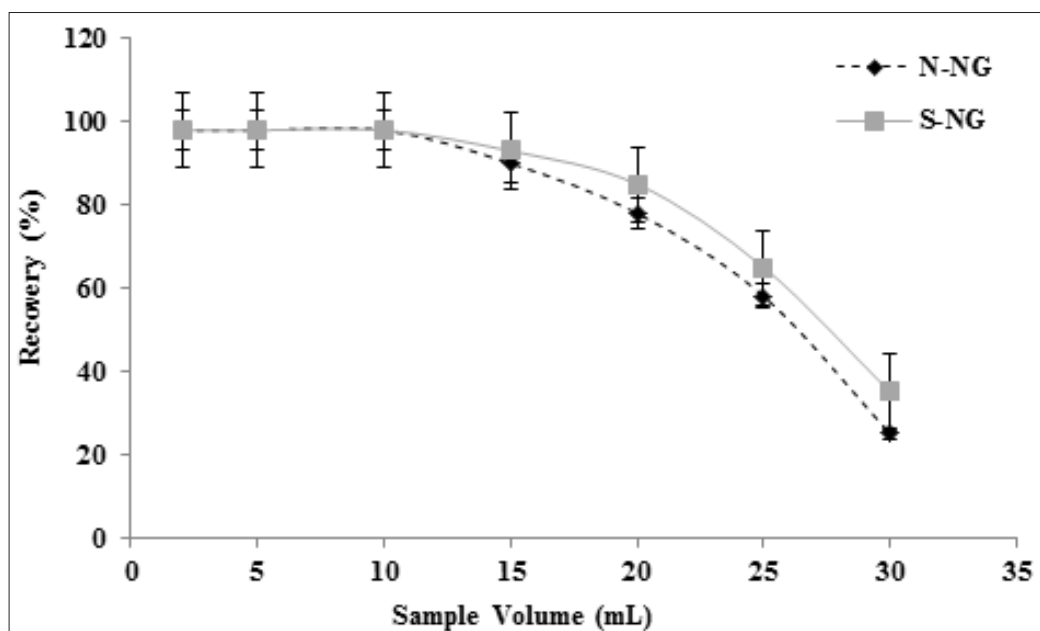
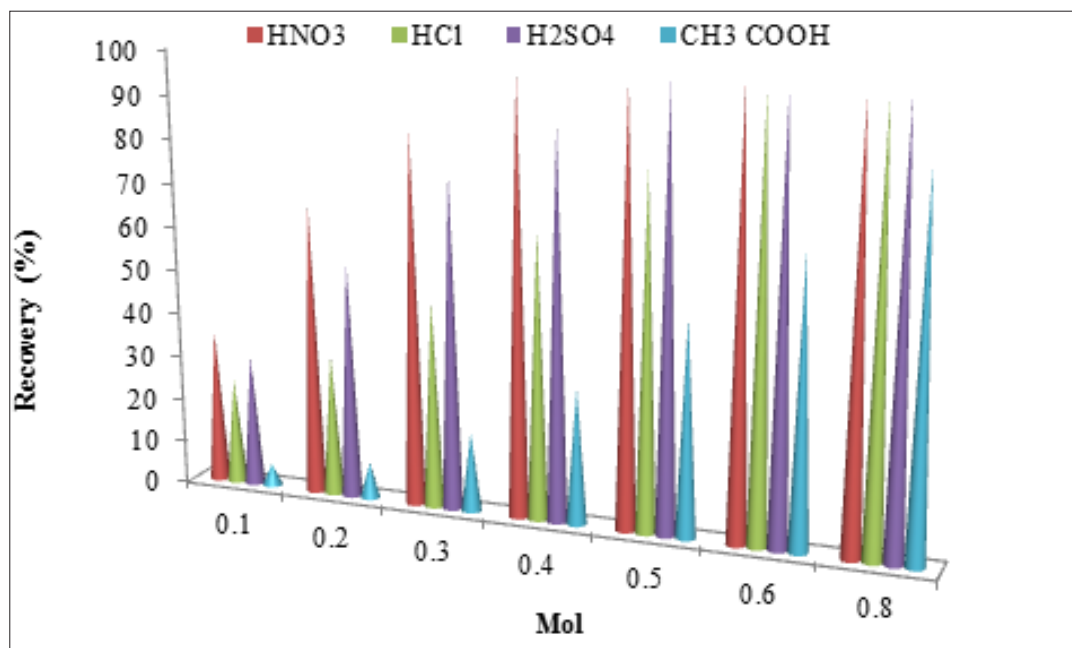


Fig. 11. The effect of sample volume on chromium extraction by FNG



**Fig. 12.** The effect of inorganic and organic acids on Cr(III) back extraction by S-NG

optimized conditions, 80 mg of [HMIM][PF<sub>6</sub>] had more efficiency for chromium extraction by procedure (Fig. 13).

The SMSPE method based on S-NG, N-NG was used for real samples, the interference of some coexisting ions encountered in water samples on the recovery of Cr (III) ions was investigated in optimized condition. This procedure was performed by adding various amounts of the interfering ions to

10 mL of standard sample solution containing 2.5  $\mu\text{g L}^{-1}$  of Cr (III) and Cr(VI). The results showed, the most of the concomitant had no considerable effect on chromium extraction (less than 5%).

### 3.6. Validation of speciation chromium by FNG

The chromium complexation was evaluated with different modified graphene as novel Nano-materials by SMSPE method. The analysis of

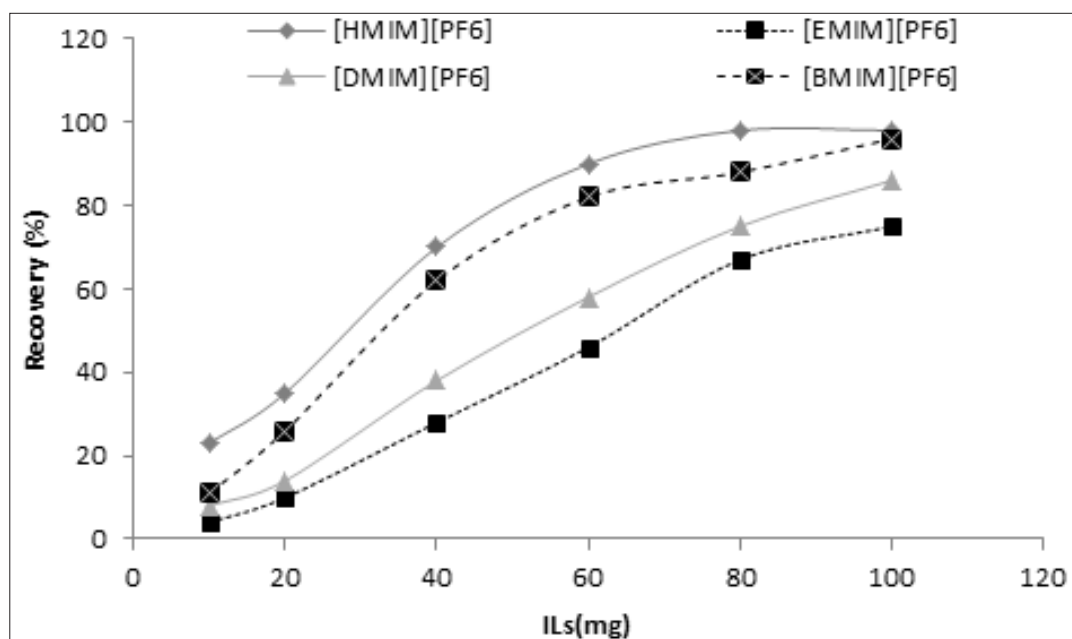


**Fig. 13.** The effect of different ILs on chromium extraction by FNG

chromium was validated by spiking chromium standard solution to real water samples. Based on result; S-NG is good adsorbent for chromium extraction by SPE. The SMSPE procedure was used for trace chromium analysis in water and wastewater samples. The experimental results based on average of three determinations, for Cr (III) were achieved in real water samples. For evaluation, real samples in standard and water samples was validated by chromium spiking to real samples (Table 5). The good recovery and accuracy with

S-NG was achieved by proposed method in water and wastewater samples. The mean recoveries of spiked samples were satisfactory obtained at 98.6%. Also, The high recovery with N-NG was achieved for Cr (VI) by proposed method in water and wastewater samples. The recoveries of spiked samples were satisfactory obtained more than 95% (Table 6).

#### 4. Conclusions

NG and FNG was synthesis and used for chromium

**Table 5.** Validation of SMSPE method based on S-NG /IL by spiking of mercury standard concentration in water samples ( $\mu\text{g L}^{-1}$ )

Sample	Added	Found <sup>a</sup>	Recovery (%)
	Cr (III)	Cr (III)	Cr (III)
Drinking Water	-----	0.17 ± 0.01	-----
	0.2	0.38 ± 0.02	105
	0.4	0.56 ± 0.04	97.5
River Water	-----	1.04 ± 0.05	-----
	1.0	1.99 ± 0.09	95
	1.5	2.47 ± 0.12	96.3
Wastewater	-----	0.88 ± 0.04	-----
	1.0	1.89 ± 0.10	101
	1.5	2.36 ± 0.12	98.6
Wastewater*	-----	1.22 ± 0.05	-----
	1.0	2.19 ± 0.11	97
	2.0	3.15 ± 0.14	96.5

<sup>a</sup> Mean of three determinations ± confidence interval (P= 0.95, n=10)

\* Wastewater diluted with DW 1:10

**Table 6.** Validation of SMSPE method based on N-NG /IL by spiking of mercury standard concentration in water samples ( $\mu\text{g L}^{-1}$ )

Sample	Added	Found <sup>a</sup>	Recovery (%)
	Cr (VI)	Cr (VI)	Cr (VI)
Tab Water	-----	0.113 ± 0.014	-----
	0.1	0.209 ± 0.017	96.0
	0.2	0.315 ± 0.026	101.1
Well Water	-----	0.503 ± 0.025	-----
	0.5	0.997 ± 0.048	98.8
	1.0	1.498 ± 0.073	99.5
Wastewater of petrochemical factory	-----	1.011 ± 0.057	-----
	0.5	1.495 ± 0.074	96.8
	1.0	2.033 ± 0.096	102.2
Wastewater of color factory	-----	0.954 ± 0.044	-----
	0.5	1.443 ± 0.063	97.8
	1.0	1.938 ± 0.121	98.4

<sup>a</sup> Mean of three determinations ± confidence interval (P= 0.95, n=10)

extraction (CrIII, CrVI) in water samples by SMSPE procedure. An effective function treatment was reported for graphene by using KPS as oxidant in alkaline media to prepare graphene stable solution. The atomic structure in the functional groups, as well as their method and mechanism of their stabilization on graphene, are two essential factors that can determine the phenomenon in graphene nanofluids. Surface and amine modification of graphene based on SMSPE was used for separation/preconcentration of Cr(III) and Cr(VI) in waters, respectively. The results showed us, the surface modification of graphene has a strong influence on the dispersion stability, thermal conductivity of NG and help to chemically adsorption of chromium speciation. The FNG (S-NG and N-NG) can be extracted chromium in different pH by physical and chemical adsorption. All of FNG such as SDBS-GNSs, K-GNSs, SDBS-KGNS, A-GNSs, SDBS-AGNS, N-GNSs and S-GNSs can be extracted chromium with different recovery by proposed method. The results showed, N-GNSs ( $Cr_{VI}$ ) and S-GNSs ( $Cr_{III}$ ) had more efficient recovery for chromium extraction from waters by chemical adsorption. The developed method based on N-GNSs and S-GNSs was low interference, simple and easy preparation, low RSD% and high precision /recoveries for chromium speciation/extraction in water and wastewater samples (more than 96%).

## 5. References

- [1] C. He, Z. Yang, J. Ding, Y. Chen, X. Tong, Y. Li , Effective removal of Cr(VI) from aqueous solution by 3-aminopropyltriethoxysilane-functionalized graphene oxide. *Colloid Surf. Physicochem. Eng. Asp.*, 520 (2017) 448–458.
- [2] L. Wang., D. Han., J. Luo, Li T., Z. Lin., Y. Yao, Highly efficient growth of boron nitride nanotubes and the thermal conductivity of their polymer composites, *phys. Chem. C*, 122 (2018) 1867-1873.
- [3] C.T. Hsieh, Y.F. Chen, C.E. Lee, Y.M. Chiang, H. Teng, Thermal transport in stereo carbon framework using graphite nanospheres and graphene nanosheets, *Carbon*, 106 (2016) 132-141.
- [4] A.B. Showkat, A. Tariq, A. Moheman, Z. Ngaini, Functionalized graphene nanocomposites for water treatment, functionalized graphene nanocomposites and their derivatives synthesis, processing and applications micro and nano technologies, Chapter 5 (2019) 98-107
- [5] H.J. Salavagione, M.A. Gomez, G. Martinez, Polymeric modification of graphene through esterification of graphite oxide and poly(vinyl alcohol), *Macromol.*, 42 (2009) 6331-6334.
- [6] L. Sun , T. Wang , M. Wu , Z. Wang , Y. Yang , G. Pan , Inhibiting the corrosion-promotion activity of graphene, *Chem. Mater.*, 27 (2015) 2367-2373.
- [7] B. Ramezanzadeh, S. Niroumandrad, A. Ahmadi, M. Mahdavian, M.H. Mohamadzadeh, Enhancement of barrier and corrosion protection performance of an epoxy coating through wet transfer of amino functionalized graphene oxide, *Corros. Sci.*, 103 (2016) 283-304.
- [8] Y.C. Seong, K. Minsu, K. Min, L. Min, K. Bum Kim, Effect of Cu surface treatment in graphene growth by chemical vapor deposition, *Mater. Lett.*, 236 (2019) 403-407
- [9] S. Li, K. Tu, C. Lin, C.W. Chen, Chhowalla M., Solution-processable graphene oxide as an efficient hole transport layer in polymer solar cells, *ACS Nano*, 4 (2010) 3169-3174.
- [10] M. Lotya, Y. Hernandez, P.J. King, R.J. Smith, Nicolosi V., Karlsson L.S., Liquid phase production of graphene by exfoliation of graphite in surfactant/water solutions, *Am. Chem. Soc.*, 131 (2009) 3611-3620.
- [11] P. Liang, H. Sang, Speciation of chromium in water samples with cloud point extraction separation and preconcentration and determination by graphite furnace atomic absorption spectrometry, *J. Hazard. Mater.*, 154 (2008) 1115–1119.
- [12] H Shirkhanloo, M Ghazaghi, HZ Mousavi, Chromium speciation in human blood samples based on acetyl cysteine by dispersive liquid–liquid biomicroextraction and in-vitro evaluation of acetyl cysteine/cysteine for decreasing of hexavalent chromium concentration, *J. pharm. Biomed. Anal.*, 118 (2016) 1-8.
- [13] A. Zhitkovich, Importance of chromium-DNA adducts in mutagenicity and toxicity of chromium

- (VI), *Chem. Res. Toxicol.*, 18 (2005) 3–11.
- [14] M.S. Hosseini, F. Belador, Cr(III)/Cr(VI) speciation determination of chromium in water samples by luminescence quenching of quercetin, *J. Hazard. Mater.*, 165 (2009) 1062–1067
- [15] A. Ghizatloo, M. Shariaty-Niasar, A.M. Rashidi, Preparation of nanofluids from functionalized Graphene by new alkaline method and study on the thermal conductivity and stability, *Int. Commun. Heat Mass*, 42 (2013) 89–94.
- [16] W. Guoxiu, Y. Juan, J. Park, G. Xinglong, B. Wang, H. Liu, J. Yao, Facile synthesis and characterization of graphene nano sheets, *Phys. Chem. C*, 112 (2008) 192–195.
- [17] L. Luqi, Z. Shuang, H. Tengjiao, G. Zhi-Xin, Solubilized multi walled carbon nanotubes with broadband optical limiting effect, *Chem. Phys. Lett.*, 359 (2009) 191–195.
- [18] T.M. McCoy, G. Turpin, M. Teo, R.F. Tabora, Graphene oxide: surfactant or particle, *curr. Opin. in colloid interface Sci.*, 39 (2019) 98–109.
- [19] L. Jiang, L. Gao, J. Sun, Production of aqueous colloidal dispersions of carbon nanotubes, *Colloid Interface Sci.*, 260 (2003) 89–94.
- [20] O. Park, T. Jeevananda, N.H. Kim, S. Kim, L.J. Hee, Effects of surface modification on the dispersion and electrical conductivity of carbon nanotube/polyaniline composites, *Scripta Mater.*, 60 (2009) 551–554.
- [21] J.Y. Hye, H.K. Kyoung, K.Y. Santosh, W.C. Jae, Effects of carbon nanotube functionalization and annealing on crystallization and mechanical properties of melt-spun carbon nanotubes/poly(ethylene terephthalate) fibers, *Composites Sci. Technol.*, 72, (2012) 1834–1840
- [22] S. Safari Kish, A.M. Rashidi, H.R. Aghabozorg, L. Moradi, Increasing the octane number of gasoline using functionalized carbon nanotubes, *Appl. Surf. Sci.*, 256 (2010) 3472–3477.
- [23] H. Yuseon, I.M. Hyungu, K. Jooheon, The effect of sulfonated graphene oxide on sulfonated poly membrane for direct methanol fuel cells, *Membrane Sci.*, 425 (2012) 11–22.
- [24] C.A. Dyke, J.M. Tour, Covalent functionalization of single-walled carbon nanotubes for materials applications, *Phys. Chem.*, 108 (2004) 151–159.
- [25] Y. Rike, O. Holia, S. Sudirman, S. Yukie, I. Tadahisa, I. Jun, Analysis of functional group sited on multi-wall carbon Nanotube surface, *The Open Mater. Sci.*, 5 (2011) 242–247.
- [26] H. Aria, Z. Büyükmumcub, T. Özpozanb, Vibrational spectroscopic study of isotopic effect on  $TcX^{3+}$  and  $TcX_3OH$  (X: O, S and Se) by DFT, *Mol. Structure*, 1165 (2018) 259–266.
- [27] C. Li, J. Lin, S. Huang, J. Lee, C. Chen, A new and acid exclusive method for dispersing carbon multi walled nanotubes in aqueous suspensions, *Colloids Surf. A: Physicochem. Eng. Aspects*, 297 (2007) 275–281.
- [28] R. Wang, H. Fan, W. Jiang, G. Ni, Amino-functionalized graphene quantum dots prepared using high-softening point asphalt and their application in  $Fe^{3+}$  detection, *App. Surf. Sci.*, 467 (2019) 446–455.
- [29] J. Paredes, S. Villar-Rodil, A. Martinez-Alonso, J.M.D. Tascon, Graphene oxide dispersions in organic solvents, *Langmuir*, 24 (2008) 560–566.
- [30] V. G. Kravets, A.N. Grigorenko, R.R. Nair, P. Blake, S. Anissimova, K.S. Novoselov, Spectroscopic ellipsometry of graphene and an exciton-shifted van Hove peak in absorption, *Phys. Rev. B*, 81 (2010) 413–422.
- [31] S. Vadukumpully, J. Paul, N. Mahanta, S. Valiyaveetil, Flexible conductive graphene/poly(vinyl chloride) composite thin films with high mechanical strength and thermal stability, *Carbon*, 49 (2011) 198–211.
- [32] S. Ganguli, A.K. Roy, D.P. Anderson, Improved thermal conductivity for chemically functionalized exfoliated graphite/epoxy composites, *Carbon*, 46 (2008) 806–812.
- [33] X.B. Sun, P. Ramesh, M.E. Itkis, E. Bekyarova, R.C. Haddon, Dependence of the thermal conductivity of two-dimensional graphite nanoplatelet-based composites on the nanoparticle size distribution, *Phys. Condens Mat.*, 22 (2010) 4216–4223.
- [34] T.S. Munonde, N.W. Maxakato, P.N. Nomngongo, Preconcentration and speciation of chromium species using ICP-OES after ultrasound-assisted magnetic solid phase extraction with an amino-modified magnetic nanocomposite prepared from  $Fe_3O_4$ ,  $MnO_2$  and  $Al_2O_3$ , *Microchim. Acta*, 184

(2017)1223–1232.

- [35] H. Peng, N. Zhang, M. He, B. Chen, B. Hu, Simultaneous speciation analysis of inorganic arsenic, chromium and selenium in environmental waters by 3-(2-aminoethylamino) propyl trimethoxysilane modified multi-wall carbon nanotubes packed microcolumn solid phase extraction and ICP-MS, *Talanta*, 131 (2015) 266–272
- [36] A. Sheikhmohammadi, S.M. Mohseni, R. Khodadadi, M. Sardar, M. Abtahi, S. Mahdavi, H. Keramati, Z. Dahaghin, S. Rezaei, M. Almasian, M. Sarkhosh, M. Faraji, S. Nazari (2017) Application of graphene oxide modified with 8-hydroxyquinoline for the adsorption of Cr (VI) from wastewater: Optimization, kinetic, thermodynamic and equilibrium studies, *J. Mol. Liq.*, 233 (2017) 75–88.
- [37] X. Qia, S. Gao, G. Ding, A.N. Tang, Synthesis of surface Cr (VI)-imprinted magnetic nanoparticles for selective dispersive solid-phase extraction and determination of Cr (VI) in water samples, *Talanta*, 162 (2017) 345–353.